ISSN 1541-308X, Physics of Wave Phenomena, 2017, Vol. 25, No. 2, pp. 140–146. © Allerton Press, Inc., 2017.

MAGNETIC RESONANCE IMAGING

Optimization of MRI Parameters for the Gradient Echo Method in Fluorocarbon Research

N. V. Anisimov[1*], M. V. Gulyaev[1], D. V. Volkov[2***], S. S. Batova[2****], O. S. Pavlova[2*****], D. V. Fomina[2******], and Yu. A. Pirogov[2*******]**

[1] *Faculty of Fundamental Medicine, Lomonosov Moscow State University, Lomonosovsky pr. 31/5, Moscow, 119991 Russia*

[2] *Faculty of Physics, Lomonosov Moscow State University, Leninskie Gory 1, str. 2, Moscow, 119991 Russia*

Received July 19, 2016

Abstract—The problems of magnetic resonance imaging (MRI) of objects having a very wide spectrum of the nuclear magnetic resonance, where signals from all its lines are difficult to detect, have been investigated. It is proposed to carry out MRI using frequency-selective pulses. A method for setting optimally the pulse parameters and the start time of induction signal detection is described. The calculation results are compared with the MRI data obtained for a fluorocarbon compound.

DOI: 10.3103/S1541308X1702011X

1. INTRODUCTION

Fluorocarbon compounds (FCCs) are applied in medicine as drugs, gas-transport preparations, and contrast agents [1]. Since they do not contain hydrogen atoms, the in vivo study of their properties by nuclear magnetic resonance (NMR) is based on the ^{19}F NMR methods [1, 2]. At 100% natural content, the gyromagnetic ratio of fluorine atom, γ, is only 6% smaller than that of proton; therefore, the ^{19}F NMR sensitivity ($\sim\gamma^3$) is only 13% lower than that for ^{1}H NMR.

An important feature of ^{19}F MRI is the absence of background signal from normal tissues because the fluorine content in them is very low. In addition, using ^{19}F MRI, one generally does not need to apply scanning techniques aimed at differentiating tissues with respect to their relaxation times because in most cases the task is to determine the localization of only one preparation. This circumstance simplifies the choice of MRI parameters of a scanning pulse sequence.

It is convenient to assign ^{19}F MRI images with anatomical structures using ^{1}H MRI images. The assignment is significantly simplified if ^{19}F and ^{1}H MRI images are obtained in identical scanning geometries.

FCC ^{19}F NMR spectra often contain many lines with chemical shifts Δ covering a wide range: up to several hundreds ppm. In magnetic fields of 1 T and higher, the corresponding absolute values are $\Delta \sim 10^3 - 10^4$ Hz. This circumstance imposes more stringent requirements on the instrumental resources as compared with proton MRI, where the main contribution to the recorded signal is from water and fat, whose chemical shifts differ by only 3.5 ppm.

Stringent requirements are imposed on the RF oscillator. Indeed, the RF pulses must be sufficiently short to excite the entire NMR spectrum ($t_\mathrm{p} < 1/\Delta$). At the same time, they must have a sufficiently high power to rotate the magnetization vector by a large flip angle FA (flip angle is the rotation angle of the magnetization vector for nuclear spins under the effect of RF pulse) because $\mathrm{FA} = \gamma B_1 t_\mathrm{p}$, where B_1 is the RF pulse amplitude. Let us estimate the power P that must be supplied to a cavity with a diameter D from a transmitter with an output resistance $R = 50\,\Omega$ in the case $\mathrm{FA} = \pi$. Since the cavity is a high-Q contour tuned to the Larmor frequency $\omega = \gamma B_0$ (B_0 is the magnetic field induction), its matching with the output transmitter yields $\omega L = R$, where L is the contour inductance. Using the Ohm law $I = U/R$, where I is a current through the contour and U is a voltage across the contour, and the Faraday law $LI = B_1 S$, where $S = \pi D^2/4$, and assuming that $t_\mathrm{p} = 1/\Delta$, we arrive at $P = U^2/2R$, where $U = \pi^2 B_0 \Delta D^2/4$.

*E-mail: anisimovnv@mail.ru
**E-mail: mihon-epsilon@ya.ru
***E-mail: mdanf@gmail.com
****E-mail: teka-kor@yandex.ru
*****E-mail: oleuf@mail.ru
******E-mail: dv.fomina@physics.msu.ru
*******E-mail: yupi937@gmail.com

For example, if a 7-T scanner is equipped with a 1-kW power transmitter and a cavity with an operating diameter of 10 cm, which can work at the same power, the pulse sequence spin echo (SE) with 180°-pulses can be implemented only at $\Delta < 3$ kHz.

These limitations are not so urgent for the pulse sequence gradient echo (GE), where 180°-pulses are not used, and the spin system can be excited at small FA values. However, the recorded signal is weaker in this case, not only because FA is small but also because the induction signal is attenuated by the beginning of the signal recording due to the interference of spin packets, which represent individual spectral components. Therefore, the time of echo (TE) delay (the time of echo is the interval between the triggering of the RF pulse used to excite the spin system and the instant of recording the response from it) should be as minimal as possible for the GE technique.

The parameter Δ determines also the requirements to the power and switching speed of the gradient system, because it is necessary to perform not only RF excitation of the spin system but also spatial coding of the Larmor frequencies (to obtain finally the MRI image) during the interval $\sim 1/\Delta$. The requirements to the gradients are reduced to the formula $G_{\max} > 2\pi\Delta/\gamma d$, where d is the spatial resolution (with respect to the size of scanned voxel or, in the case of slice-to-slice scanning, slice thickness). In particular, if a scanner is equipped with a gradient system characterized by $G_{\max} = 0.1$ T m^{-1}, the resolution $d = 1$ mm for fluorine ($\gamma/2\pi = 40.06$ MHz T^{-1}) can be implemented only at $\Delta < 4.2$ kHz.

The digitization rate of this signal, characterized by bandwidth BW (the frequency range that is planned to be either excited using an RF pulse or detected), should be such as to make it digitized for the induction signal decay time ($\sim 1/\Delta$), which is rather short: $1/\Delta \ll T_2$ (T_2 is the transverse relaxation time). In the opposite case, the MR image will be distorted because of the chemical shift artifact of the first kind [3]. The requirement to BW is reduced to the inequality $\mathrm{BW} > N\Delta$, where N is the size of the MR image matrix. The N value must be more than a few tens, otherwise the image will be poorly informative.

The best of modern commercial analog-to-digital converters (ADCs) provide BWs up to 10 MHz [4]. However, standard scanners use generally less expensive devices, with BW lower by half or even more [5].

An increase in the bandwidth of the receiver is accomplished by an increase in the thermal noise at the detector input ($\sim \Delta^{1/2}$), with a corresponding loss of sensitivity.

Note also the problem related to the chemical shift artifact of the second kind: dependence of the MRI signal on TE. This dependence is generally difficult to calculate; however, the main problem is the significant decrease in the signal intensity after the time interval $\sim 1/\Delta$. The technical possibilities of reducing TE are rather limited. The TE value is mainly determined by the durations of RF and gradient pulses (including the rise time) and the induction signal acquisition time.

The SE method is used to overcome this problem, which makes it possible to recover (using a refocusing 180°-pulse) the induction signal after a time interval TE to the same value as after the excitation pulse. The recovery is not quite complete because of transverse relaxation. Nevertheless the SE method appears to be preferred as compared with GE.

Actually available equipment does not always make it possible to obtain 180°-pulses of desired duration and power. Note also that the SE signal can be weakened because of the J-modulation effects, which, in contrast to the chemical-shift effects, cannot be eliminated using a refocusing pulse. The presence of additional delays for this pulse in the SE sequence does not make it possible to implement a scan rate as high as in the GE method. Therefore, the GE method can be called for in individual MRI applications.

The requirements to instrumental resources become more stringent when passing to stronger magnetic fields B_0. Stronger fields are called for because the MRI sensitivity in weak fields is insufficiently high due to the low FCC concentration: FCCs are used in the form of diluted emulsions because of their hydrophobic properties. At the same time, in view of the fact that the excretion time for many FCCs is long (several months or more), the preparation doses introduced into human organism (even in the form of emulsions) must be limited.

An increase in B_0 is accompanied by a proportional rise in the B_1 and $G_{\max}$ values. Since these values are proportional to the currents flowing through the transfer and gradient coils, both transmitter power and gradient strength rise proportionally to $\sim B_0^2$.

Since these instrumental requirements cannot be satisfied in all cases, compromise solutions are sought for when carrying out ^{19}F MRI.

The instrumental requirements can be made less stringent by passing from broadband to frequency-selective excitation of the spin system. This approach allows one to reduce the parameter Δ. The problem is that in this case not all spectral lines contribute to the MRI signal, as a result of which the method may become insufficiently sensitive. Therefore, it is necessary to find a version of selective excitation (the

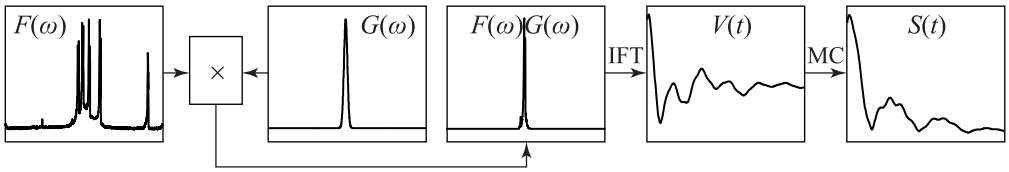

Fig. 1. Schematic of the calculation of the MRI signal in the case of selective excitation over the spectrum obtained upon broadband excitation.

central frequency position and the spectral width Δf) in which the recorded signal is maximum.

Frequency selection of excited spins can be implemented by appropriate choice of the RF pulse parameters. However, in this case one must do it without slice-to-slice (2D) scanning, where a slice-coding gradient is applied to localize cuts synchronously with the RF pulse. A necessary condition for this spin localization technique is that the spectral band of the RF pulse is wider than the NMR spectrum.

This problem does not exist for 3D scanning, because in this case slice-to-slice representation of images is obtained after reconstructing phase coding data along two orthogonal directions, and the spin excitation can in principle be performed without applying a slice-coding gradient. This gradient serves to limit the total scanning volume to avoid, in particular, aliasing in the image along the second direction of phase coding. However, if there are no potential signal sources beyond the scanned area, there is no need in applying this gradient.

2. EXPERIMENTAL

The GE MRI scan parameters are analyzed by determining the selective excitation version providing the maximum signal. The essence of the method is to determine (based on the NMR data) the maximum induction signals for different versions of selective excitation of the spin system. To this end, it is proposed to obtain plots emulating the induction signals formed by selective excitation. Their time forms are generated using the reverse Fourier transform, applied to the previously edited NMR spectrum. The editing is reduced to multiplication of the initial spectrum by the excitation profile. The positions of extrema in the thus obtained plots are used as landmarks for setting the TE parameter, which determines the instant of GE signal formation. Using the diagram with subordination of extreme values, one can choose a version with maximum induction signal and use specifically this version to obtain MRI images.

For simplicity, we will apply the method to small FA values. In this case, one can obtain simple calculation relations between the pulse spectrum and the excitation profile for the spin system, because this profile is determined by the Fourier transform of the pulse envelope at small FA [6, 7]. In addition, the effect of relaxation factors can be neglected when analyzing the pulse sequence. Finally, the experimental verification of the method is simplified, because the requirements to the power of the transmitter and gradient system become less stringent.

For definiteness, we consider a Gaussian pulse; in this case, the RF pulse length is minimized in comparison with the pulses of other shapes at a specified spectral width; this circumstance, in turn, is favorable for TE minimization.

The method is implemented as follows. The initial NMR spectrum $F(\omega)$ is multiplied by a Gaussian function $G(\omega)$ with specified width and spectral localization, and the multiplication result is subjected to inverse Fourier transform (IFT). The quadrature components $U(t)$ and $V(t)$ obtained as a result of this transform are used to calculate the signal magnitude from the formula $S(t) = \sqrt{U(t)^2 + V(t)^2}$ (Fig. 1). Based on the plot $S = S(t)$, one can estimate the signal intensity in the magnitude MRI image, if TE is set to be t in MRI.

The necessary calculations (multiplication of the spectrum by the Gaussian function, inverse Fourier transform, calculation of the magnitude, etc.) and scanning of the K space were performed using homemade software, operating on the PC platform in the MS Windows® environment [8].

An experimental approval of the method was performed with a 7-T MR imager Bruker BioSpec 70/30 USR, equipped with ParaVision 5 software and electronic equipment AVANCE, including the following components: gradient system BGA-20SA (at a current of 100 A, $G_{\max} = 105\,\mathrm{mT\,m^{-1}}$ and the rate of gradient rise is $300\,\mathrm{T(m\,s^{-1})^{-1}}$, 1-kW RF transmitter BLAH 1000, cavity T10334 with an inner diameter of 7.2 cm (modified so as to detect not only ^{1}H but also ^{19}F signals and capable of operating at an RF power up to 750 W [9]), and an ADC HADC/2 with a digitization rate up to 1 MHz.

The method was approved on the fluorocarbon compound perfluorodecalin. This is one of the main components of the Perftoranum® preparation, which is authorized for application in medicine. This prepa-

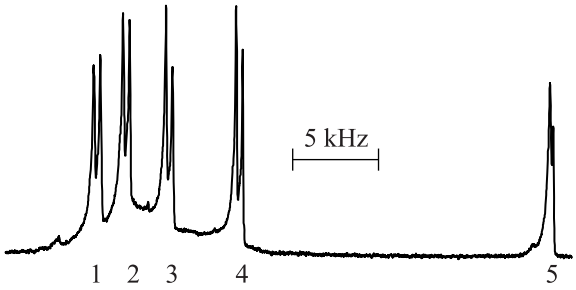

Fig. 2. Part of perfluorodecalin spectrum. The enumerated fragments and the regions combining two and more fragments are used for selective excitation.

ration has gas-transport properties and is used as a blood substitute for this reason [10].

A conventional ^{19}F NMR spectrum with a width of about 45 kHz was recorded for perfluorodecalin. A rectangular 13-μs pulse was applied to this end, after which the induction signal was read with digitization of 8K points. To smooth the noise, the induction signal $S_0(t)$ was multiplied by the exponential $S(t) = S_0(t)\exp(-LBt\pi)$ (where $LB = 10$ Hz) before the Fourier transform. The above-described algorithm was used to calculate the induction signal for a number of selective excitation versions, in which the Gaussian function width Δf was varied from 1.4 to 23 kHz.

Figure 2 shows a part of the perfluorodecalin spectrum with the strongest lines [11]. Five (enumerated) fragments can clearly be distinguished. These fragments, as well as spectral regions containing two and more of them, were chosen for selective excitation. In particular, these are regions containing fragments 1 and 2, 2 and 3, 3 and 4, from 1 to 3, from 2 to 4, from 1 to 4, and from 1 to 5. These combinations are enumerated below by numbers from 6 to 12. The same numbers denote selective excitation versions. When selecting the latter, their practical validity was taken into account. In particular, the versions requiring a large spectral width with a small number of spectral lines (for example, the excitation of the pair of distant peaks 4 and 5) were rejected.

3. RESULTS

We calculated signals for all 12 versions of selective excitation. Figure 3 shows the calculation results for three of them. A normalization is performed with respect to the maximum value of the signal for version 12. In all versions the maximum values of signals lie near $t = 0$. However, because of technical limitations, the TE values could not be set shorter than 2.86 ms. The limitations are determined by the RF pulse duration ($\simeq 1-2$ ms), the gradient pulse duration (0.7 ms), the rise time of the gradient pulse (0.3 ms), and the induction signal reading time (0.32 ms). Therefore, we are interesting in only the maxima located after 2.86 ms. In particular, for version 5, the extremum in the vicinity of $t \simeq 6.4$ ms is of interest. In all other versions, the strongest signal peaks (along with that at $t = 0$) are located near $t \simeq 3.2$ ms.

The calculation data make it possible to predict the extreme values of induction signals for any selective excitation version. It is important that one can reveal the subordination of signals for the chosen versions of selective excitation and determine the time TE necessary to implement it at MRI scanning. This approach simplifies the search for the optimal MRI parameters.

We experimentally verified the calculation results by measuring the mean values of signals in the MRI images of an ampoule filled with perfluorodecalin, which were obtained by the 3D GE method. The main parameters of the scanning pulse sequence were as follows: repetition time TR = 600 ms, FA = 30°, BW=200 kHz, Echo Position = 50, Matrix = $N_{\rm f} \times N_{\rm p1} \times N_{\rm p2} = 64 \times 67 \times 8$, and FOV = $4.76 \times 5.0 \times 3.2$ cm. The ADC used in our scanner can perform digitization up to BW = 1 MHz. However, as practice showed, its operation becomes somewhat unstable with BW set above 200 kHz: artifacts of the background illumination line type arose in the MRI images; this situation generally corresponds to detector zero drift. Therefore, the BW values were generally chosen below 200 kHz.

The induction signal digitization time in each stage of phase coding was $N_{\rm f}/{\rm BW} = 32 \times 10^{-5}$ s = 0.32 ms, and the total scanning time was $N_{\rm p1} \times N_{\rm p2} \times {\rm TR} = 0.6 \times 67 \times 8 = 321.6$ s ≈ 5 min 22 s. The duration $t_{\rm p}$ of the Gaussian pulse formed with an amplitude cutoff at a level of 0.01 was set proceeding from the relation $t_{\rm p} = 2.74/\Delta f$, where Δf is the spectral width at the $1/e$ level. The factor is chosen to be 2.74 because this value is the product of the spectral widths Δf and Δt for the Gaussian functions

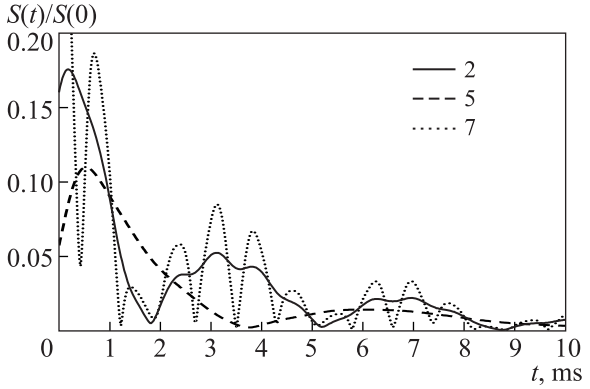

Fig. 3. Plots of calculated MRI signals for three versions of selective excitation of perfluorodecalin.

Calculated and experimental data for different selective excitation versions

Version (No.)	Δf, kHz	$M(0)/M_{\max}(0)$	$t_{\max}$, ms		$M(t_{\max})/M_{\max}(0)$	
		Theory	Theory	Experiment	Theory	Experiment
1	1.4	0.165	3.09	3.10	0.296	0.206
2	1.4	0.176	3.13	3.15	0.338	0.312
3	1.4	0.155	3.11	3.20	0.308	0.245
4	1.4	0.147	3.20	3.25	0.338	0.262
5	1.4	0.058	6.06	6.5	0.080	0.104
6	3.0	0.322	3.13	3.18	0.544	0.571
7	3.2	0.292	3.18	3.27	0.508	0.498
8	4.8	0.308	3.22	3.22	0.498	0.468
9	5.1	0.470	3.15	3.25	0.746	0.825
10	6.4	0.454	3.20	3.25	0.707	0.671
11	8.4	0.639	3.20	3.25	0.925	0.950
12	23.0	1	3.20	3.25	1 (0.157)	1

defined on an infinite interval, with Δf defined at a level of $1/e$ and Δt defined at a level of $1/2$. The latter condition, in combination with the specified cutoff level, is determined by manufacturer's settings for the envelope of a real (limited in time) Gaussian pulse set in a tabular form.

Note that manufacturer's formula $t_{\rm p} = 2.74/\Delta f$ suggests that the width Δf is measured at half maximum rather than at a level of $1/e$ [12]. The reason is that the manufacturer's specified calculations are oriented to FA = 90°. This angle is far from small; therefore, the excitation profile does not coincide with the pulse Fourier transform in this case. The Bloch equations must be solved to calculate it. This calculation shows that the profile somewhat differs from Gaussian (in particular, is somewhat wider). It remains bell-shaped, and more significant distortions (transformation into a two-humped curve) begin with somewhat larger angles: FA > 116°. We set FA to be 30°, i.e., analyzed the case of small angles, where the excitation profile coincides with the pulse Fourier transform (i.e., is also Gaussian) and the relations between Δf and Δt can easily be calculated analytically. Then manufacturer's formula for calculating $t_{\rm p}$ from a specified Δf value remains valid, but Δf should be considered as the width measured at a level of $1/e$. This circumstance was taken into account when setting the calculation values of Δf.

MRI measurements were performed with setting the same values of the spectral width and RF values as for the calculation versions. Since the subordination of amplitude values was violated for some versions, we performed additional MRI measurements with variation in TE to search for the maximum value of the MRI signal. As a result, the experimentally determined TE values were found to somewhat exceed the calculation ones: by 0.1 ms (3%) for all versions except for 6, where this difference was larger but did not exceed 7%.

The table contains the relative values of extreme intensities for different selective excitation versions and the points $t = t_{\max}$ at which the corresponding plots $M(t)$ pass through these values.

The intensities were normalized to the maximum signal for version 12. The M values for t near zero are compared in the third column, and the most intense extrema for the other t values are compared in the sixth column. One can see that the latter are concentrated mainly in the vicinity of $t \simeq 3.2$ ms, except for version 5, where the extremum is located at $t \simeq 6$. In addition, the $M(t_{\max})/M(0)$ ratio for version 12 is given in parentheses.

The table contains both the calculation and experimental data. MRI signals were measured at different TE values, and the TE values corresponding

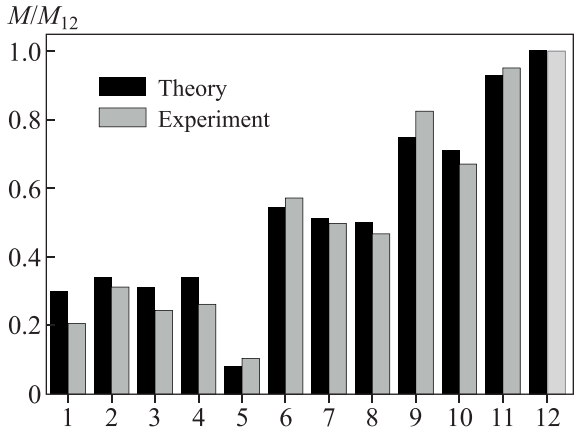

Fig. 4. Extreme values of signals for different selective excitation versions.

to maximum signals were fixed (the fifth column of table). The seventh column of the table contains the magnitudes of these signals normalized to the MRI signal magnitude that turned out to be maximum for all selective excitation versions. To compare the calculation and experimental results, the data from columns 6 and 7 are also presented in the form of diagrams (Fig. 4).

4. ANALYSIS OF THE RESULTS

One can note that both calculated and experimental data yield qualitatively identical subordinations of extreme signals for different versions of selective excitation. The signal amplitudes differ by no more than 15%, and the difference for the TE values does not exceed few percent.

One of the factors affecting the measurement accuracy was the shift of the GE signal: the echo was formed in our experiments before it was programmed in the scanning pulse sequence. As a result, the Echo Position parameter is not equal to the declared value of 50, which corresponds to a symmetric (with respect to the center of the K space) echo plot but to about 30, a value at which TE decreases by about 0.06 ms in comparison with its programmed value. This effect was found when analyzing the structure of the K space. Possible reasons for the GE signal shift, along with program errors, are technical shortcomings, e.g., unbalanced amplitudes of frequency-coding gradient pulses, responsible for the echo formation.

Another factor that may be responsible for the discrepancy between the experimental and calculation data is the broadening of lines in the initial spectrum because of the preliminary treatment: multiplication of digitized induction signal by a decaying exponential. The same effect may be due to the inhomogeneity of the field B_0. It can be shown that, if the extrema in the plot of the magnitude signal are positioned at $t = T$, broadening of the spectral line by δ should shift these extrema to smaller t values by $\delta T^2/\pi$. In our case, $T \simeq 3.2$ ms and $\delta \simeq 10$ Hz; thus, the corresponding shift is 0.033 ms.

The total contribution of the aforementioned factors yields a shift of 0.093 ms, which is in good agreement with a difference of about 0.1 ms, revealed when comparing the calculated and experimental data (see the table).

Note one more factor that may affect the calculation results: the first-order phase correction. If the initial induction signal is subjected not only to a Fourier transform but also to a first-order phase correction, the IFT yields as a result an induction signal shifted along the time axis with respect to the prototype. The phase correction is necessary because the induction signal is generally detected with some delay, caused by technical factors (setting a pause necessary to damp the ringing in the transmitter pulse, etc.). The shift of the reading onset for signal $S(t)$ by t_0 is equivalent to the replacement of $S(t)$ with $S(t-t_0)$ and its Fourier transform $F(\omega)$ with $\exp(-\omega t_0)\,F(\omega)$. The first factor in the expression for the Fourier transform determines the frequency modulation of the spectrum, due to which its phase-sensitive transform becomes too complicated for visual perception. To solve this problem, one should either deal with the magnitude spectrum or apply the first-order phase correction: multiplication of the spectrum by the function $\exp(\omega\alpha)$, where the α value is chosen so as to make the spectrum conventional. Obviously, this can be done only at $\alpha = t_0$. The IFT of the phase-corrected spectrum yields a time transform shifted by t_0. A problem is that the results of fitting α to t_0 may be somewhat different in different sessions of phase correction (subjective factor of manual correction or use of different automatic correction algorithms); this circumstance introduces variability in determining the time positions of calculated plots.

The effect of this factor should be minimized by calculating all versions of selective excitation at identical parameters of phase correction or by completely excluding it when manipulating with the initial data. Note that not all the programs aimed at processing NMR spectra provide for the latter approach.

5. APPLICATION OF THE ALGORITHM FOR THE SPIN ECHO TECHNIQUE

The results of the induction signal calculation can also be called for when planning the SE pulse sequence. To this end, one can use the plots obtained for induction signals in the following way: to mark on them the instant of applying the refocusing 180°-pulse; reproduce (starting from this point) the initial fragment of the plot inverted in time; and, finally, add the initial fragment. In sum, one obtains a spin echo pattern, in which induction signal fragments available for detection can be seen; these fragments, corresponding to the time points $t = 0$, cannot be recorded by the GE method.

Implementation of the SE method is hindered by the difficulties in generating broadband 180°-pulses. With the equipment used by us, they could be obtained for only versions 1–5, where $\Delta f = 1.4$ kHz. For version 6, which calls for $\Delta f = 3$ kHz, a 180°-pulse with this band cannot be generated because the transmitter power is insufficiently high. Even when a rectangular pulse is used instead of Gaussian, Δf is no wider than 2.87 kHz. Note that the pulse shape is of little importance for spin refocusing; the main requirement is that its excitation profile must be not narrower than that of the excitation pulse.

Therefore, when calculating the selective excitation parameters, one can set the limiting (technically attainable) Δf values for a rectangular pulse and perform a computation for only these values.

It is possible that the future development of the corresponding technologies will allow to implement other selective excitation versions, e.g., those where two or more uncoupled spectral fragments are simultaneously excited. However, even then the calculation method proposed here will be called for.

We are planning to improve our algorithm for calculating selective excitation parameters by setting an automatic enumeration of the RF value and, possibly, by varying the excitation bandwidth. In this case, a multidimensional data array is formed, whose processing is reduced to searching for the maximum signal value and reporting the coordinates of this signal: TE values, RF value of the excitation pulse, and its excitation profile (frequency spectrum).

6. CONCLUSIONS

The proposed method for optimizing MRI parameters, which is based on the analysis of different versions of frequency-selective excitation of spin system, makes it possible to obtain (using relatively simple calculation tools) acceptable results for planning MRI experiments when the object studied has a complex NMR spectrum and the instrumental resources are limited.

ACKNOWLEDGMENTS

This study was supported by the Ministry of Education and Science of the Russian Federation (Grant No. 14.604.21.0060 (RFMEFI60414X0060)).

REFERENCES

1. Ruiz-Cabelloa J., B.P. Barnett, P.A. Bottomley, and J.W.M. Bulte, "Fluorine (^{19}F) MRS and MRI in Biomedicine," NMR Biomed. **24**, 114 (2011).
2. I. Tirotta, V. Dichiarante, C. Pigliacelli, G. Cavallo, G. Terraneo, F.B. Bombelli, P. Metrangolo, and G. Resnati, "^{19}F Magnetic Resonance Imaging (MRI): From Design of Materials to Clinical Applications," Chem. Rev. **115**(2), 1106 (2015).
3. E.M. Haacke, R.W. Brown, M.R. Thompson, and R. Venkatesan, *Magnetic Resonance Imaging: Physical Principles and Sequence Design* (Wiley, N.Y., 1999).
4. www.jeolusa.com/PRODUCTS/Nuclear-Magnetic-Resonance/JNM-ECZR
5. www.bruker.com/products/mr/preclinical-mri/biospec/technical-details.html
6. M. Veshtort and R.G. Griffin, "High-Performance Selective Excitation Pulses for Solid- and Liquid-State NMR Spectroscopy," ChemPhysChem. **5**, 834 (2004).
7. J. Pauly, D. Nishimura, and A. Makovski, "A k-Space Analysis of Small-Tip-Angle Excitation," J. Magn. Res. **81**, 43 (1989).
8. N.V. Anisimov, S.S. Batova, and Yu.A. Pirogov, *Magnetic Resonance Imaging: Contrast Control and Cross-Disciplinary Application*. Ed. by Yu.A. Pirogov (MAKS Press, Moscow, 2013) [in Russian].
9. M.V. Gulyaev, L.L. Gervits, Yu.A. Ustynyuk, N.V. Anisimov, Yu.A. Pirogov, and A.R. Khokhlov, "Aquisition of Images in Magnetic Resonance Imaging on the ^{19}F Nuclea with the Help of Preparation Perftoran," J. Radio Electron. N 8 (2013) (www.jre.cplire.ru/win/aug13/11/text.html) [in Russian].
10. E.I. Maevsky and L.L. Gervits, "Perfluorocarbon-Based Blood Substitute—Perftoran. Russian Experience," Suppl. Chimica Oggi. Chem. Today, Focus on Fluorine Chemistry. **26**(3), 8 (2008).
11. C. Jacoby, S. Temme, F. Mayenfels, N. Benoit, M.P. Krafft, R. Schubert, J. Schrader, and U. Flögel, "Probing Different Perfluorocarbons for in Vivo Inflammation Imaging by ^{19}F MRI: Image Reconstruction, Biological Half-Lives and Sensitivity," NMR Biomed. **27**(3), 261 (2014).
12. Bruker-BioSpin, Shaped RF Pulses PV 3.0.1 Online Manual (2003), p. D-5-8.